

A Compact Ultra-Wideband Circularly Polarized Antenna Array for Vehicular Communications

Wei He^{1,2}, Yejun He^{2,*}, Long Zhang², Jun Hong¹, Haixia Cui³, Amir Boag⁴

¹ School of Electrical and Information Engineering, Hunan Institute of Technology, Hengyang 421002, China

² College of Electronics and Information Engineering, Shenzhen University, Shenzhen 518060, China

³ School of Physics and Telecommunication Engineering, South China Normal University, Guangzhou 510630, China

⁴ School of Electrical Engineering, Tel Aviv University, Tel Aviv 69978, Israel

* The corresponding author, email: heyejun@126.com

Cite as: W. He, Y. He, *et al.*, "A compact ultra-wideband circularly polarized antenna array for vehicular communications," *China Communications*, vol. 20, no. 6, pp. 310-320, 2023. DOI: 10.23919/JCC.fa.2021-0579.202306

Abstract: In this paper, a new compact ultra-wideband (UWB) circularly polarized (CP) antenna array for vehicular communications is proposed. The antenna array consists of a 2×2 sequentially rotated T-shaped cross dipole, four parasitic elements, and a feeding network. By loading the T-shaped cross dipoles with parasitic rectangular elements with cut corners, the bandwidth can be expanded. On this basis, the radiation pattern can be improved by the topology with sequential rotation of four T-shaped cross-dipole antennas, and the axial ratio (AR) bandwidth of the antenna also can be further enhanced. In addition, due to the special topology that the vertical arms of all T-shaped cross dipoles are all oriented toward the center of the antenna array, the gain of proposed antenna is improved while the size of the antenna is almost the same as the traditional cross dipole. Simulated and measured results show that the proposed antenna has good CP characteristics, an impedance bandwidth for $S_{11} < -10$ dB of about 106.1% (3.26:1, 1.57-5.12 GHz) and the 3-dB AR bandwidth of about 104.1% (3.17:1, 1.57-4.98 GHz), a wide 3-dB gain bandwidth of 73.3% as well as the peak gain of 8.6 dBic at 3.5 GHz. The overall size of antenna is $0.56\lambda \times 0.56\lambda \times 0.12\lambda$ (λ

refers to the wavelength of the lowest operating frequency in free space). The good performance of this compact UWB CP antenna array is promising for applications in vehicular communications.

Keywords: circularly polarized antenna; vehicle satellite communications; cross-dipole antenna; ultra-wideband (UWB) antenna

I. INTRODUCTION

Circularly polarized antennas have several important advantages compared to linear polarized ones, such as combating multi-path interferences or fading, reduced Faraday rotation and no requirement for strict orientation between transmitting and receiving antennas [1]. Therefore, CP antennas are a key technology for vehicle satellite communications [2–5]. The pursuit of high data transmission rate and large throughput in modern vehicular network systems requires the antennas to have wider bandwidth [6]. In summary, wideband and ultra-wideband (UWB) CP antennas can not only cover multiple satellite communication bands, but also increase the data transmission rate of the system. Therefore, wideband and UWB CP antennas have become an important component of vehicular communication systems. In recent years, a variety of techniques have been used to achieve wideband and UWB CP radiation, such as multi-layer patch anten-

Received: Jul. 28, 2021

Revised: Nov. 18, 2021

Editor: Guoru Ding

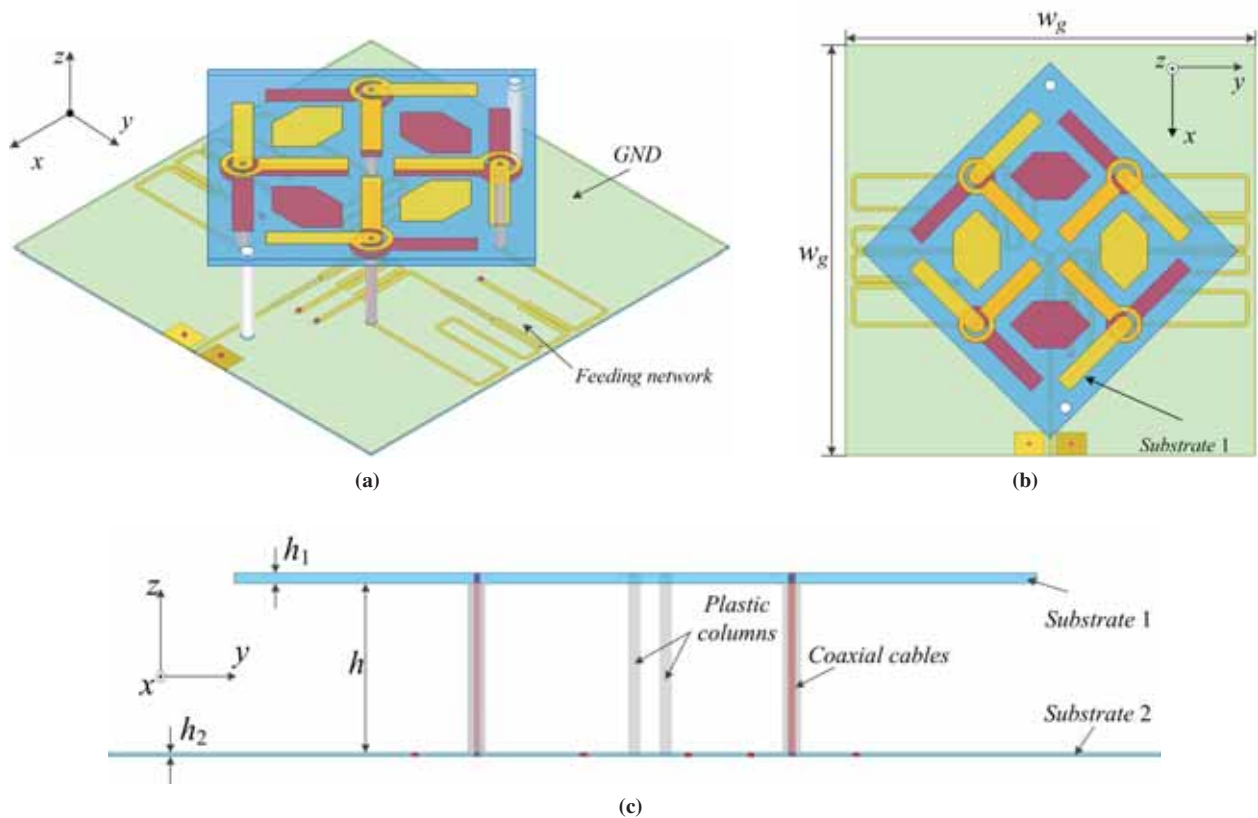


Figure 1. Geometry of the proposed antenna array: (a) 3D view; (b) Top view; (c) Side view. $h=24$ mm, $h_1=1.6$ mm, $h_2=0.508$ mm, $w_g=108$ mm.

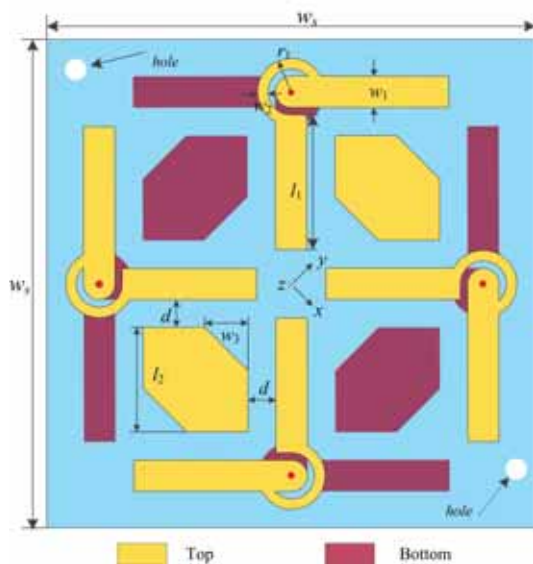


Figure 2. Top view of the top PCB with T-shaped cross dipoles and parasitic elements. $w_s=70$ mm, $w_1=4.5$ mm, $w_2=1.5$ mm, $w_3=6.2$ mm, $r_1=4.8$ mm, $l_1=19.3$ mm, $l_2=15$ mm, $d=4$ mm.

nas [7], monopole antennas with coplanar wave guide (CPW) feeding line and modified ground [8], hybrid dielectric resonator antenna [9] and antenna loaded by a metasurface [10].

In addition, the cross-dipole antenna is also an important type of wideband CP antenna [11]. A conventional cross-dipole antenna loaded with magneto-electric dipole was illustrated in [12], which could achieve a 3 dB axial ratio (AR) bandwidth of 26.8%. In [13], by loading a conventional cross-dipole antenna with an asymmetrical cross-loop, the AR bandwidth of 53.4% could be obtained. Using crossed bowtie dipole with sequentially rotated L-shaped parasitic elements was shown to broaden the AR bandwidth to 74.1% [14]. In [15], employing modified dipole arms and one parasitic patch, a 3-dB AR bandwidth of 68.6% has been obtained. Coupling multiple parasitic elements has been shown to greatly expand the AR bandwidth of the traditional cross-dipole antenna to reach 66% [16] and 72.7% [17]. Loaded with an irregular parasitic patch and pads, a conventional

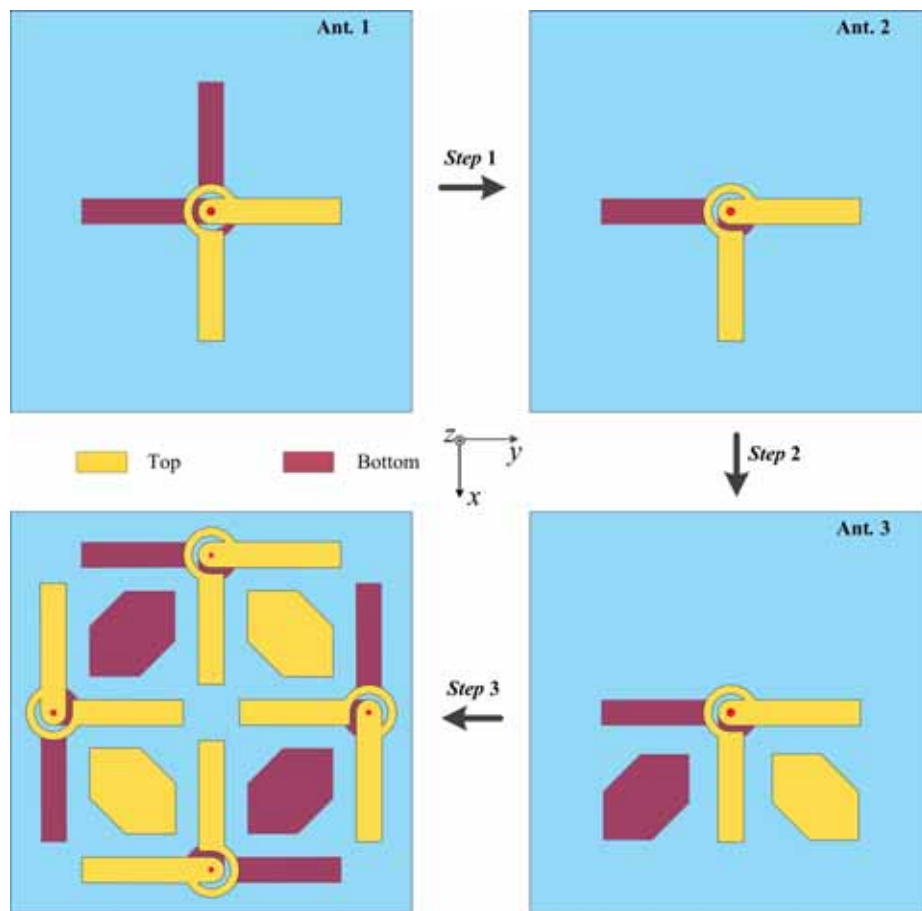


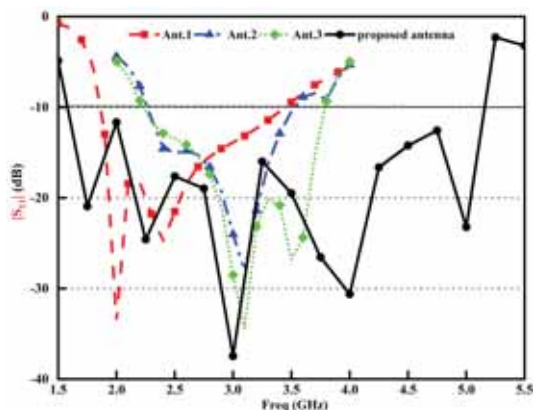
Figure 3. Antenna design evolution.

cross-dipole antenna has generated two additional resonances resulting in a wideband AR bandwidth of 85.5% [18]. Using dual-mode resonators as the arms of a cross dipole and loading multimode parasitic elements could enhance the AR bandwidth to 67.2% [19] and 94.4% [20], respectively. Although the aforementioned methods achieve wideband or UWB CP radiation, the structures are not compact, and the overall size exceeds one wavelength. Using meandering dipole arms [21], or with an artificial magnetic conductor (AMC) instead of the traditional reflector [22] and adding parasitic plates rotationally on reflector [23] has been shown to reduce the size of the antennas, but at the expense of their operating bandwidths.

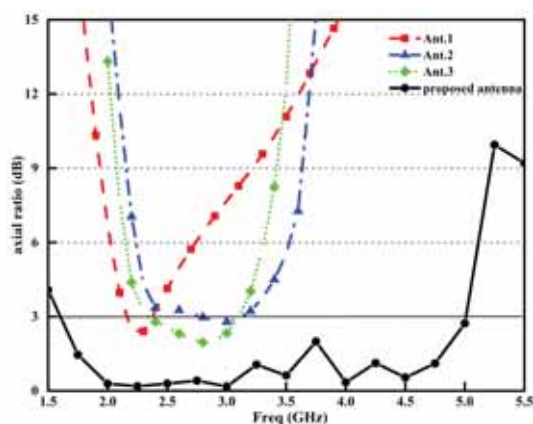
Recently, a compact T-shaped cross-dipole antenna produced by rotating half of the cross dipole by 90° and a folded E-shaped antenna obtained by bending the arms of the T-shaped cross dipole were proposed [24]. The size of these antennas could be miniaturized to almost half of the traditional cross-dipole an-

tenna, but the operating bandwidths were very narrow. What's more, due to the asymmetry in the overall structure, the radiation patterns deteriorate.

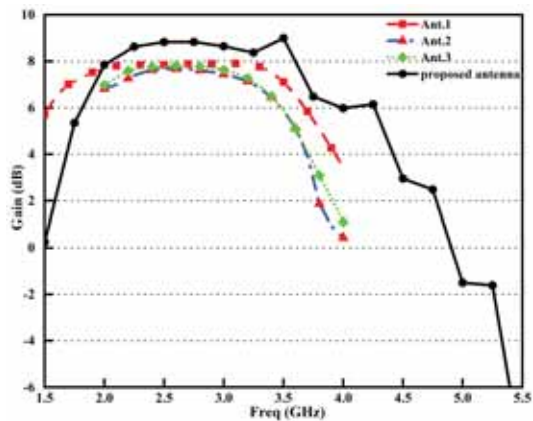
In this paper, a compact UWB CP antenna array for vehicular communications is proposed. The proposed antenna achieves an impedance bandwidth for $S_{11} < -10$ dB of about 106.1% (3.26:1, 1.57-5.12 GHz) and the 3-dB AR bandwidth of about 104.1% (3.17:1, 1.57-4.98 GHz), which covers L-band, S-band and part of C-band, and its overall size is only $0.56\lambda \times 0.56\lambda \times 0.12\lambda$. Firstly, adding two parasitic rectangular elements with cut corners to the T-shaped cross dipole, the bandwidth can be expanded. Then, by sequential rotation of four T-shaped cross-dipole antennas, and making the vertical arms of all T-shaped cross dipoles oriented toward the center of the antenna, the radiation pattern of the proposed antenna is significantly improved. Moreover, when adding a wideband feeding network and 90° sequential phase shifting, the operating bandwidth is greatly enhanced as well. Due



(a)



(b)

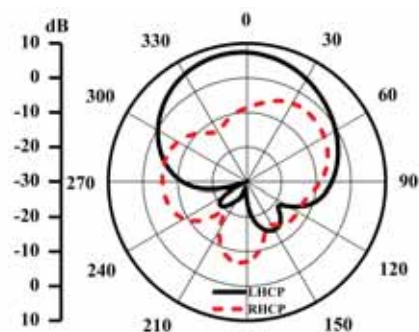


(c)

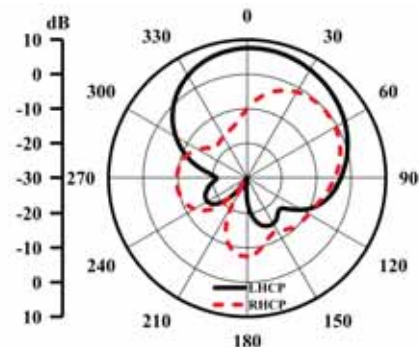
Figure 4. The simulated results of different antennas: (a) $|S_{11}|$; (b) AR; (c) Gain.

to the special topology of the proposed antenna array, the structure is very compact, and the size is almost the same as that of the single traditional cross dipole.

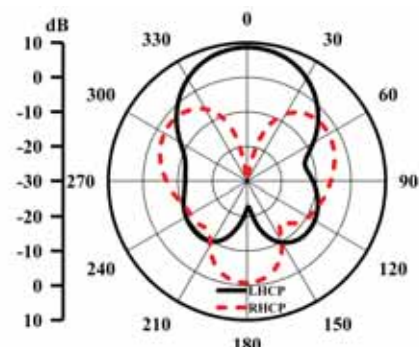
II. ANTENNA DESIGN AND ANALYSIS



(a)



(b)



(c)

Figure 5. The simulation radiation pattern of different antennas at 3 GHz. (a) T-shaped cross dipole, (b) T-shaped cross dipole with parasitic elements, (c) Proposed antenna.

Figure 1 shows the configuration of the proposed compact UWB CP antenna array. As shown, the antenna array consists of two PCBs, four feeding coaxial cables and two supporting plastic columns. The material of the top PCB is FR4, and its thickness is 1.6 mm (h_1), and four T-shaped cross dipoles and four parasitic elements are printed on the top and bottom surfaces. The material of bottom PCB is Rogers 4003, and its thickness is 0.508 mm (h_2), and a wideband feeding network and a reflector are printed on the bot-

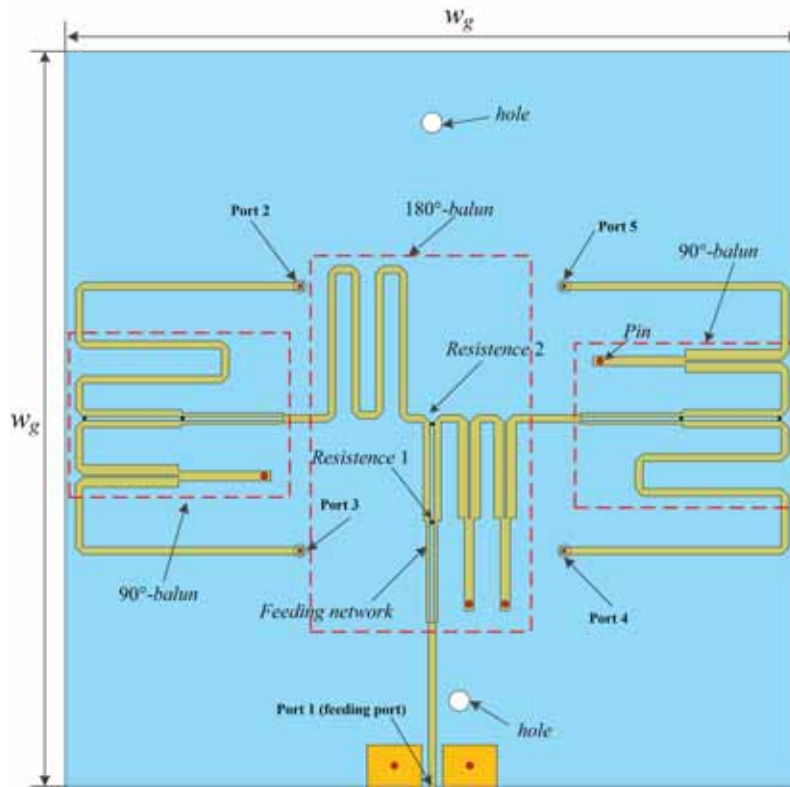


Figure 6. Antenna feeding network.

tom and top surfaces, respectively. The distance between the two PCBs is 24 mm (h).

2.1 Sequential Rotation Compact T-Shaped Cross-Dipole Antenna (Top PCB)

Figure 2 shows the top view of top PCB, and its size is $w_s \times w_s$. Four T-shaped cross dipoles and four parasitic elements with cut corners are printed with sequential rotation on the two side of top PCB. In the proposed topology, the vertical arms of each T-shaped cross dipole are placed toward the center of the antenna, which makes the structure of the antenna very compact. Each parasitic element has the same coupling distance (d) with the adjacent dipole arm. Two parasitic elements are printed on the top surface of the substrate, while the other two are printed on the bottom one.

The proposed antenna design process is shown in Figure 3. The three steps are as follows:

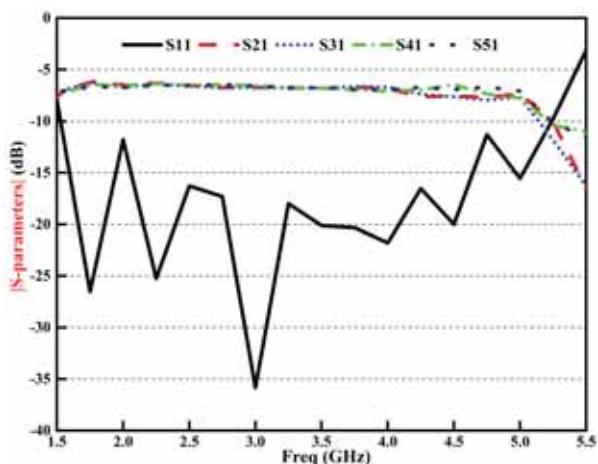
Step 1: Rotate half of the traditional cross dipole (Ant. 1) by 90° to obtain the T-shaped cross dipole (Ant. 2), which has been described in detail in [24]. According to [24], the impedance bandwidth of T-

shaped cross dipole is decreased, and the radiation pattern is tilted.

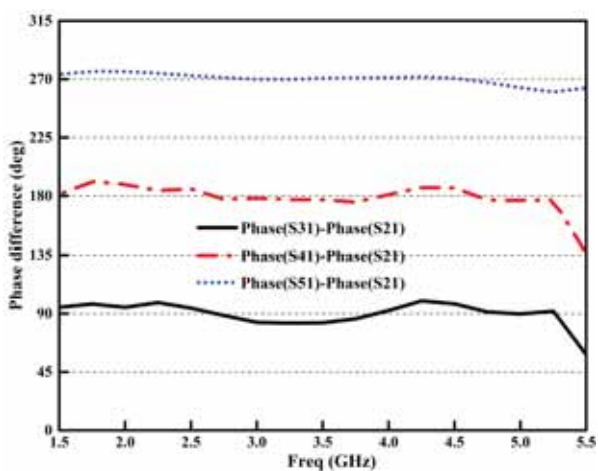
Step 2: In order to improve the operating bandwidth of T-shaped cross dipole, two parasitic elements with cut corners are coupled between the arms of the T-shaped dipole (Ant. 3). However, the radiation pattern is still tilted.

Step 3: Rotate the four T-shaped cross dipoles and the four parasitic elements in sequence, and direct the vertical arms of each T-shaped cross dipole toward the center of the antenna, thus a very compact UWB CP antenna can be obtained. The overall size of the proposed antenna is almost the same as the traditional cross-dipole antenna. This special topological form can not only improve the radiation patterns of the T-shaped cross dipole, but also can greatly expand the impedance bandwidth and AR bandwidth.

The performance of Ant. 1-3 and that of the proposed antenna are shown in Figures 4 and 5, where a reflector of the same size is placed under each antenna, and the parameters of each antenna are optimized to the best value. As shown in Figure 4, the impedance bandwidth of Ant. 2 is 43.4% (2.27-3.53 GHz), which



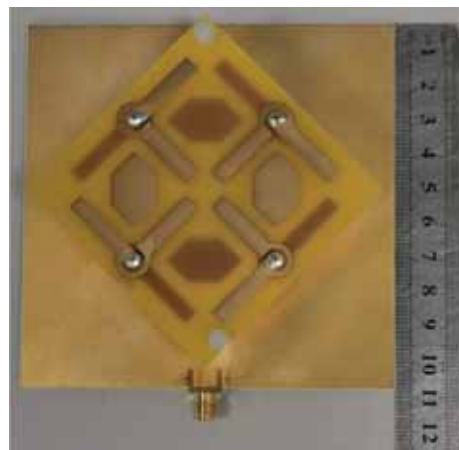
(a)



(b)

Figure 7. Simulated results of the feeding network: (a) $|S|$ – parameters and (b) Phase difference of these four ports.

is lower by 16.2% compared with the impedance bandwidth of Ant. 1 (59.6%:1.86-3.44 GHz), while the AR bandwidth is almost the same being 9.8% (Ant. 2: 2.9-3.21 GHz) and 9.3% (Ant. 1: 2.16-2.37 GHz), respectively. These are consistent with the aforementioned analysis. From Figure 5, one can see that transition from Ant. 1 to Ant. 2 causes the radiation pattern to deteriorate and become tilted. When two parasitic elements are coupled to Ant. 2, the impedance bandwidth and AR bandwidth of the antenna are improved, which is in good agreement with the previous analysis. The impedance bandwidth and AR bandwidth of Ant. 3 are 51.8% (2.23-3.79 GHz) and 27.9% (2.34-3.1 GHz), respectively. However, the radiation pattern is still tilted. In addition, Figure 5 also illustrates that the radiation



(a)



(b)

Figure 8. Prototype of the proposed antenna. (a) top view, (b) bottom view.

pattern is improved by rotating four T-shaped cross dipoles and four parasitic elements according to the topology in Figure 3. As shown in Figure 4, in this case, the impedance bandwidth and AR bandwidth of the antenna are greatly expanded, and the gain is also increased by about 1dB.

2.2 1 to 4 Feeding Network (Bottom PCB)

The bottom view of feeding network is shown in Figure 6. The size of this feeding network is $w_g \times w_g$. This feeding network has an UWB power divider and stable phase difference performance, and consists of a 180° out-of phase balun and two 90° baluns, which are designed in [25, 26]. The simulation results of the feeding network are illustrated in Figure 7. The impedance

Table 1. Comparison between the proposed antenna and other kinds of wideband and UWB CP antenna. (λ refers to the wavelength of the lowest operating frequency in free space)

Ref.	Antenna Type	Antenna Size (λ^3)	Impedance Bandwidth (% , GHz)	3-dB AR Bandwidth (% , GHz)	3-dB Gain Bandwidth (% , GHz)	Peak Gain (dBic)
[7]	Slot antenna	$0.32 \times 0.35 \times 0.1$	62% (3.6-6.85)	49% (3.6-5.93)	N. G	3.3
[9]	Slot antenna with Metasurface	$0.80 \times 0.80 \times 0.05$	97.2% (2.68:1, 2.97-7.95)	83.2% (2.35:1, 3.3-7.75)	73.8% (3.5-7.45)	10.8
[13]	Cross dipole with parasitic elements	$1.01 \times 1.01 \times 0.29$	91.4% (2.68:1, 1.2-3.22)	74.1% (2.15:1, 1.37-2.95)	N. G.	9.27
[15]	Cross dipole with parasitic elements	$1.04 \times 1.04 \times 0.26$	77.6% (2.27:1, 1.11-2.52)	66% (1.98:1, 1.25-2.48)	66% (1.25-2.48)	7.2
[16]	Cross dipole with parasitic elements	$1.11 \times 1.11 \times 0.28$	99.2% (2.98:1, 1.24-3.68)	72.7% (2.14:1, 1.41-3.02)	72.7% (1.41-3.02)	10.1
[17]	Cross dipole with irregular patch	$1.17 \times 1.17 \times 0.29$	95% (2.81:1, 1.16-3.26)	85.5% (2.49:1, 1.24-3.09)	78% (1.25-2.85)	6.67
[19]	Cross dipole with multiple modes	$1.04 \times 1.04 \times 0.26$	95.5% (2.83:1, 0.92-2.60)	94.4% (2.79:1, 0.95-2.65)	94.4% (0.95-2.65)	6.8
[22]	cross dipole with parasitic plates on GND	$0.29 \times 0.29 \times 0.1$	63.2% (1.04-2)	52.4% (1.1-1.88)	N. G.	4
[25]	Sequentially rotated patch antenna	$1.13 \times 1.13 \times 0.15$	98% (2.96:1, 2-5.92)	96.3% (2.79:1, 2.16-6)	82.5% (2.65-5.95)	9.5
[26]	Monopole	$1.17 \times 1.17 \times 0.1$	132.8% (4.95:1, 1.17-5.79)	92.5% (2.72:1, 1.75-4.76)	72.3%	12.6
This Work	T-Shaped Cross Dipole	$0.56 \times 0.56 \times 0.12$	106.1% (3.26:1, 1.57-5.12)	104.1% (3.17:1, 1.57-4.98)	73.3% (1.9-4.1)	8.6

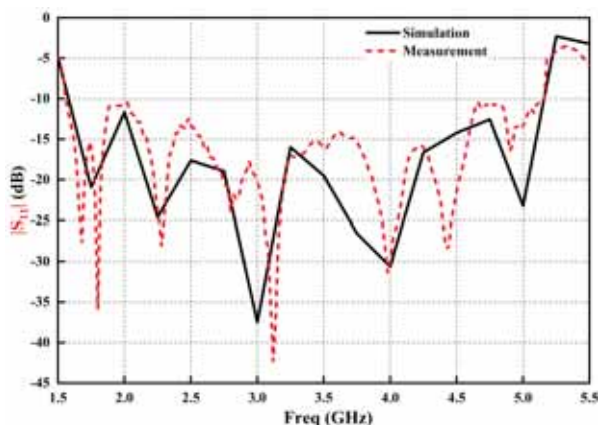


Figure 9. Simulated and measured S_{11} for fabricated antenna.

bandwidth of the feeding network with $S_{11} < -10$ dB is from 1.5 to 5.2 GHz (110.4%), and the phase difference between Port 2 and Port 3, Port 4, Port 5 is maintained at about 90° , 180° , 270° within the bandwidth of 1.5 to 5.2 GHz, respectively. The magnitude unbalance of the insertion loss is less than 1 dB.

III. RESULTS AND DISCUSSIONS

The proposed UWB compact circularly polarized antenna array was fabricated and measured to prove the correctness of the previous analysis. Figure 8 shows the photos of the fabricated antenna. The simulated

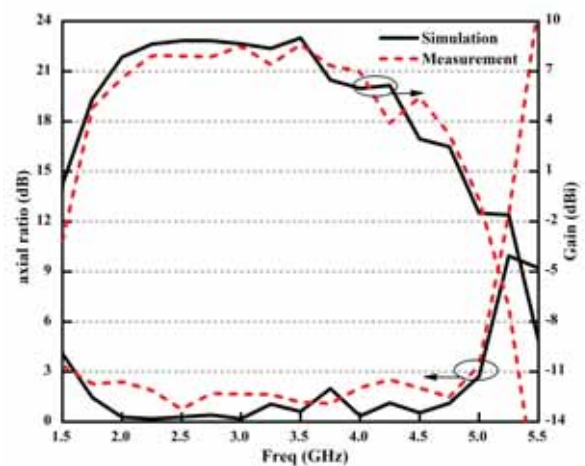


Figure 10. Simulated and measured AR and gain at broadside direction.

and measured results are shown in Figure 9. As shown, the measured impedance bandwidth of $S_{11} < -10$ dB is about 106.1% from 1.57 to 5.12 GHz, which is in agreement with the simulation result. Figure 10 indicates the measured and simulated results of AR and gain in the broadside direction. Due to the special topology of the proposed antenna and the good performance of the feeding network, the bandwidth of $AR < 3$ dB can cover the frequency range from 1.57 to 4.98 GHz, reaching 104.1% (3.17:1). As shown in

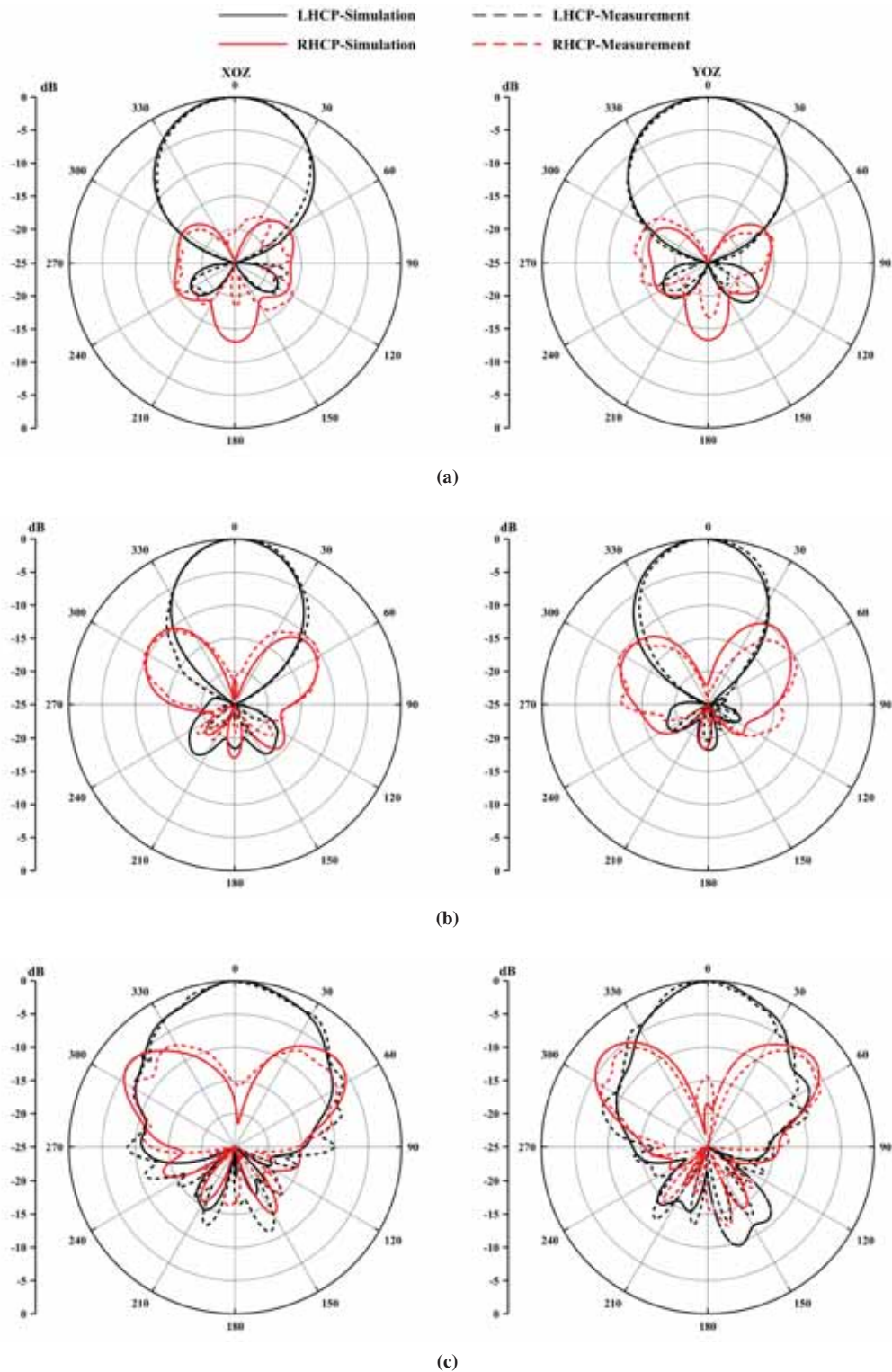


Figure 11. Simulated and measured radiation pattern for fabricated antenna at XOZ and YOZ planes. (a) 2.5 GHz, (b) 3.5 GHz, (c) 4.5 GHz.

Figure 10, the measured gain is slightly lower than the simulated gain, and the maximum gain is 8.6 dBi at 3.5 GHz. In addition, the 3-dB gain bandwidth is about

73.3% from 1.9 to 4.1 GHz, and in this band, the AR is all less than 3 dB. The measured and simulated results of radiation pattern at 2.5, 3.5, and 4.5 GHz are plotted

in Figure 11 (a), (b), and (c), respectively. The results show that the measured results are in good agreement with the simulation in the upper hemisphere region, while the results in the other hemisphere are a little different. The cause of this discrepancy maybe the reflection and scattering of the test turntable and the coaxial cable.

Table 1 shows the performance comparison between the proposed antenna and other antennas. It can be seen that the proposed antenna has wider operating bandwidth and higher gain although its overall size is larger compared to the [7] and [22]. In addition, compared to the other references in Table I, the proposed antenna not only has a very compact structure, but also has a wider 3-dB AR bandwidth. Overall, the proposed antenna has a wider operating bandwidth and a very small size.

IV. CONCLUSION

An compact ultra-wideband circularly polarized antenna array for vehicular communications is proposed in this paper. By sequentially rotating four T-shaped cross dipoles and four parasitic elements, and direct the vertical arms of all T-shaped cross dipoles toward the center of the antenna, and placing a wideband 1 to 4 feeding network under the antenna, a very compact circularly polarized antenna is obtained. The overall size of proposed antenna is $0.56\lambda \times 0.56\lambda \times 0.12\lambda$. In addition, the impedance bandwidth and AR bandwidth of proposed antenna are 106.1% (3.26:1) from 1.57 to 5.12 GHz and 104.1% (3.17:1) from 1.57 to 4.98 GHz, respectively. Compared with other reported CP antennas, the advantages of proposed antenna are wider operating bandwidth and compact structure. With these merits, the proposed antenna array is very suitable for application in modern vehicular communication systems.

ACKNOWLEDGEMENT

This work is supported in part by the National Natural Science Foundation of China (NSFC) under Grant No. 62071306, and in part by Shenzhen Science and Technology Program under Grants JCYJ202001091-13601723, JSGG20210802154203011 and JSGG-20210420091805014.

References

- [1] S. Gao, Q. Luo, *et al.*, *Circularly polarized antennas*. Wiley-IEEE Press, 2013.
- [2] Z. Zhong, X. Zhang, *et al.*, "A compact dual-band circularly polarized antenna with wide axial-ratio beamwidth for vehicle gps satellite navigation application," *IEEE Trans. Veh. Technol.*, vol. 68, no. 9, pp. 8683–8692, 2019.
- [3] R. Xu, S. Gao, *et al.*, "A reconfigurable dual-band dual-circularly polarized antenna for vehicle global navigation satellite system application," *IEEE Trans. Veh. Technol.*, vol. 69, no. 10, pp. 11 857–11 867, 2020.
- [4] J. Zhu, Y. Yang, *et al.*, "Dual-band dual circularly polarized antenna array using fss-integrated polarization rotation amc ground for vehicle satellite communications," *IEEE Trans. Veh. Technol.*, vol. 68, no. 11, pp. 10 742–10 751, 2019.
- [5] L. Wen, S. Gao, *et al.*, "Wideband dual circularly polarized antenna for intelligent transport systems," *IEEE Trans. Veh. Technol.*, vol. 69, no. 5, pp. 5193–5202, 2020.
- [6] M. Alsath, H. Arun, *et al.*, "An integrated tri-band/uwb polarization diversity antenna for vehicular networks," *IEEE Trans. Veh. Technol.*, vol. 67, no. 7, pp. 5613–5620, 2018.
- [7] W. Yang, J. Zhou, *et al.*, "Single-fed low profile broadband circularly polarized stacked patch antenna," *IEEE Trans. Antennas Propag.*, vol. 62, no. 10, pp. 5406–5410, 2014.
- [8] U. Ullah and S. Koziel, "A broadband circularly polarized wide-slot antenna with a miniaturized footprint," *IEEE Antennas and Wireless Propag. Lett.*, vol. 17, no. 12, pp. 2454–2458, 2018.
- [9] W. Yang, W. Sun, *et al.*, "Design of a circularly polarized dielectric resonator antenna with wide bandwidth and low axial ratio values," *IEEE Trans. Antennas Propag.*, vol. 67, no. 3, pp. 1963–1968, 2019.
- [10] L. Gu, W. Yang, *et al.*, "Low-profile ultrawideband circularly polarized metasurface antenna array," *IEEE Antennas and Wireless Propagation Letters*, vol. 19, no. 10, pp. 1714–1718, 2020.
- [11] Y. He, W. He, *et al.*, "A wideband circularly polarized cross-dipole antenna," *IEEE Antennas and Wireless Propag. Lett.*, vol. 13, pp. 67–70, 2014.
- [12] S. Ta and I. Park, "Crossed dipole loaded with magneto-electric dipole for wideband and wide-beam circularly polarized radiation," *IEEE Antennas and Wireless Propag. Lett.*, vol. 14, pp. 358–361, 2015.
- [13] G. Feng, L. Chen, *et al.*, "Broadband circularly polarized crossed-dipole antenna with a single asymmetrical cross-loop," *IEEE Antennas and Wireless Propag. Lett.*, vol. 16, pp. 3184–3187, 2017.
- [14] Y. Li, Z. Zhao, *et al.*, "A cavity-backed wideband circularly polarized crossed bowtie dipole antenna with sequentially rotated parasitic elements," *Progress in Electromagnetics Research Letters*, vol. 79, pp. 1–7, 2018.
- [15] Z. Guo, Z. Zhao, *et al.*, "A directional circularly polarized crossed-dipole antenna with bandwidth enhancement," *Microwave and Optical Technology Letters*, vol. 60, no. 9, pp. 2161–2167, 2018.
- [16] L. Wang, W. Fang, *et al.*, "Wideband circularly polarized cross-dipole antenna with parasitic elements," *IEEE Access*, vol. 7, pp. 35 097–35 102, 2019.
- [17] Z. Zhao, Y. Li, *et al.*, "Design of wideband circularly polarized crossed-dipole antenna using parasitic modified

- patches," *IEEE Access*, vol. 7, pp. 75 227–75 234, 2019.
- [18] Z. Zhao, Y. Li, *et al.*, "Design of broadband circularly polarized antenna via loading coupled rotated dipoles," *Microwave and Optical Technology Letters*, pp. 425–430, 2018.
- [19] X. Liang, J. Ren, *et al.*, "Wideband circularly polarized antenna with dual-mode operation," *IEEE Antennas and Wireless Propag. Lett.*, vol. 18, no. 4, pp. 767–770, 2019.
- [20] L. Wang, W. Fang, *et al.*, "Broadband circularly polarized cross-dipole antenna with multiple modes," *IEEE Access*, vol. 8, pp. 66 489–66 494, 2020.
- [21] S. X. Ta, H. Choo, *et al.*, "Planar, lightweight, circularly polarized crossed dipole antenna for handheld uhf rfid reader," *Microwave and Optical Technology Letters*, vol. 55, no. 8, pp. 1874–1878, 2013.
- [22] Q. Chen, H. Zhang, *et al.*, "A metasurface-based slit-loaded wideband circularly polarized crossed dipole antenna," *International Journal of Rf and Microwave Computer Aided Engineering*, vol. 28, no. 1, 2017.
- [23] H. Zhang, Y. Guo, *et al.*, "A design of wideband circularly polarized antenna with stable phase center over the whole gnss bands," *IEEE Antennas and Wireless Propag. Lett.*, vol. 18, no. 12, pp. 2746–2750, 2019.
- [24] K. Kedze, H. Wang, *et al.*, "Design of a reduced-size crossed-dipole antenna," *IEEE Trans. Antennas Propag.*, vol. 69, no. 2, pp. 689–697, 2021.
- [25] Q. Liu, Z. Chen, *et al.*, "Compact ultrawideband circularly polarized weakly coupled patch array antenna," *IEEE Trans. Antennas Propag.*, vol. 65, no. 4, pp. 2129–2134, 2017.
- [26] R. Xu, S. Gao, *et al.*, "Analysis and design of ultrawideband circularly polarized antenna and array," *IEEE Trans. Antennas Propag.*, vol. 68, no. 12, pp. 7842–7853, 2020.

Biographies



Wei He received the B.S. degree in electronic and information engineering from the Hunan University of Science and Technology, Xiangtan, Hunan, China, in 2010, and the M.S. and Ph.D. degree in Information and Communication Engineering from Shenzhen University, Shenzhen, China, in 2014 and 2021, respectively. He is currently a Lecturer with the School of Electrical and Information Engineering, Hunan Institute of Technology, Hengyang, China. His current research interests include RFID tag antennas, circularly polarized antennas, and metasurface.



Yejun He received the Ph.D. degree in information and communication engineering from Huazhong University of Science and Technology (HUST), Wuhan, China, in 2005. Since 2011, he has been a Full Professor with the College of Electronics and Information Engineering, Shenzhen University, Shenzhen, China, where he is the Director of Guangdong Engineering Research Center of Base Station Antennas and Propagation, and the Director of Shenzhen Key Laboratory of Antennas and Propagation, Shenzhen, China. He was awarded as Pengcheng Scholar Distinguished Professor, Shenzhen, China in 2020. He was selected as a Fellow of IET in 2016 and the Chair of IEEE Antennas and Propagation Society-Shenzhen Chapter in 2018. His research interests include wireless communications, antennas and radio frequency.



Long Zhang received the B.S. and M.S. degrees in Electrical Engineering from the Huazhong University of Science and Technology (HUST), Wuhan, China, in 2009 and 2012, respectively, and the Ph.D. degree in electronic engineering from the University of Kent, Canterbury, U.K, in 2017. He is currently an Assistant Professor with the College of Electronics and Information Engineering, Shenzhen University, Shenzhen, China. His current research interests include circularly polarized antennas and arrays, mm-wave antennas and arrays, phased arrays, tightly coupled arrays, and reflect arrays.



Jun Hong received the B. S. degrees in applied physics from Xiangtan University, Xiangtan, China in 2003, and received the M. S. degrees in communication and information system from Ningbo University, Ningbo, China in 2009, respectively. He received the Ph.D. degree in electronic science and technology in 2013 at the school of Electronic Science and Engineering, Southeast University, Nanjing, China. He is currently a researcher with Hunan Institute of Technology, Hengyang, Hunan, China. His current research interests focus on optical and microwave communication, microwave photonics.



Haixia Cui received the M.S. and Ph.D. degrees in Communication Engineering from South China University of Technology (SCUT), Guangzhou, China, in 2005 and 2011, respectively. She is currently a Full Professor with the school of Physics and Telecommunication Engineering, South China Normal University (SCNU), China. From July 2014 to July 2015, she visited the Department of Electrical and Computer Engineering, the University of British Columbia (UBC), as a Visiting Associate Professor. Her research interests are in the areas of cooperative communication, wireless resource allocation, 5G/6G, and antennas.



Amir Boag received the B.Sc. degree in electrical engineering and the B.A. degree in physics in 1983, both Summa Cum Laude, the M.Sc. degree in electrical engineering in 1985, and the Ph.D. degree in electrical engineering in 1991, all from Technion - Israel Institute of Technology, Haifa, Israel. From 1991 to 1992 he was on the Faculty of the Department of Electrical Engineering at the Technion. From 1992 to 1994 he has

been a Visiting Assistant Professor with the Electromagnetic Communication Laboratory of the Department of Electrical and Computer Engineering at the University of Illinois at Urbana-Champaign. In 1994, he joined Israel Aircraft Industries as a research engineer and became a manager of the Electromagnetics Department in 1997. Since 1999, he is with the Physical Electronics Department of the School of Electrical Engineering at Tel Aviv University, where he is currently a Professor. Dr. Boag's interests are in computational electromagnetics, wave scattering, imaging, and design of antennas and optical devices. He has published over 110 journal articles and presented more than 250 conference papers on electromagnetics and acoustics. Prof. Boag is an Associate Editor for *IEEE Transactions on Antennas and Propagation*. He is a Fellow of the Electromagnetics Academy. In 2008, Amir Boag was named a Fellow of the IEEE for his contributions to integral equation based analysis, design, and imaging techniques.